Transactions, SMiRT-23
Manchester, United Kingdom - August 10-14, 2015
Division XII, Paper ID 272

Seismic Fragility of Base-isolated Nuclear Power Plant Structures Considering Spatially Varying Ground Motions

Kaiser Ahmad[1], Mohamed A. Sayed[1] and Dookie Kim[2]

[1]Researcher, Dept. of Civil Engineering, Kunsan National University, South Korea
[2]Professor, Dept. of Civil Engineering, Kunsan National University, South Korea

ABSTRACT

The amplitudes and phases of the seismic ground motions change significantly over extended distances. Therefore, the spatial variation of ground motions has an important effect on the responses of long structures and foundations such as nuclear power plants (NPPs). The study presents the seismic fragility analysis of a base-isolated structure under the spatially varying ground motions. In this study, the base-isolated NPP with a total height of 65.8m and hemispherical dome is modelled as a lumped mass stick model. The structural NPP stick model and the nuclear island base mat are established by installing 121 lead rubber bearing (LRB) base isolation. The ground motions incoherency is performed using an isotropic frequency-dependent spatially correlation function. The seismic fragility of BI-NPP are investigated under the uniform excitation in addition to considering the spatially varying ground motions. The fragility curves are estimated for three limit states representing the design displacement of the base isolation. Thereafter this study emphasize the need of consideration of spatial variation in seismic design codes more practically for base-isolated nuclear power plants.

INTRODUCTION

In order to assess the probabilistic seismic risk of existing and under construction nuclear power plant structures fragility curves have found lots of importance from the very nineteen seventies. As fragility analysis involves the estimation of the conditional probabilities of NPP structural or any component failure for a given level of seismic ground motion. Here, analytical fragility curves in the form of a two-parameter lognormal distribution function as given in Shinozuka et al. (2000). These two-parameters (referred to as fragility parameters) are estimated through a maximized likelihood function.
S.H Kim and M.Q Feng (2003) investigated fragility curves under differential ground motion and observed that structural responses were significantly increased in several cases for bridges. In case of spatial variation the damaged bridges increased up to 2.3 times. So there have been a lot of study for bridges only. Thereafter fragility curves for BI-NPP rather than NPP considering spatial variation is relatively new and interesting too.
Besides providing an improved methodology based on site dependant response spectra to evaluate the seismic capacity of Korean NPP in the Korean peninsula, Sung gook Cho et al (2005) conducted the seismic fragility analysis of recorded ground motions in Korea of small magnitude. Having a wide ranged variation in ground motion uncertainties, BI-NPP requires investigation of seismic fragility due to strong ground motions of high magnitude combined with spatial variation.
Ali and Nadine (2014) conducted an investigation on probabilistic seismic Hazard estimation of BI-NPP under long and short period synthesized Tohoku. USNRC SRP 3.7.1 (2012) has already defined the minimum duration for analysis of NPP which should be more than 20 seconds. Regardless being subjected to earthquake of different total time duration, structural analysis for spatially varying grounds motion is much investigating in this work.
Finally, effect of spatial variability of ground motions on seismic response of base-isolated NPP was estimated for several ground motions and fragility curves were constructed using two cases of input ground motions. In the first case, the input motions were identical at the base mate of BI-NPP; in the

second case, different input motions were applied at different location of the base mat to assess the effect of spatial variability.

SIMULATION OF GROUND MOTION WITH SPATIAL VARIATION

Selected ground motions

According to USNRC SRP 3.7.1 Revision 4 (2012) for nonlinear structural analysis minimum number of earthquake should be greater than 4. Average value of the response may be used if at least seven nonlinear time history analysis are performed. Otherwise the maximum value (i.e., envelope) of the individual responses from the multiple time history should be used. Therefore in this work we selected seven earthquakes from PEER NGA strong motion database and simulated spatially correlated earthquake ground motions at 50 m interval using the known ground motion inputs by SIMQKE II .The following table 1 gives the number of earthquakes and their details which contains the name of earthquakes, station name, magnitude, distance of epicentre, shear wave velocity and duration of earthquakes.

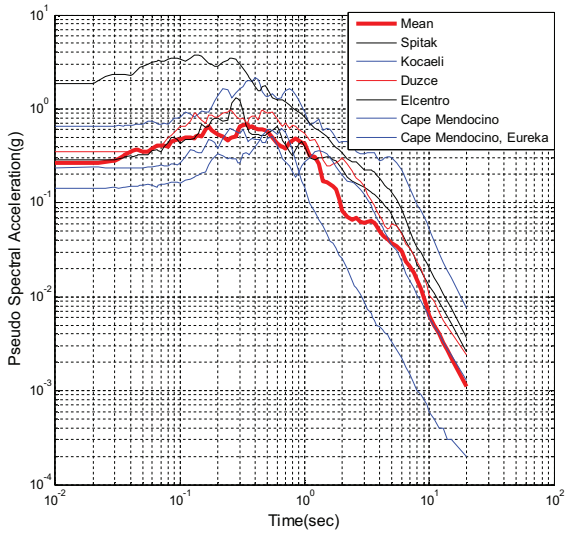

Figure 1. (a) Response spectrum of the selected ground motions (5% damping).

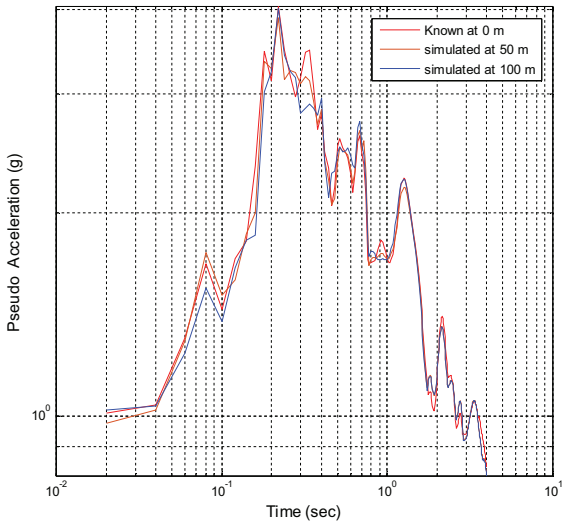

Figure 1. (b) Response spectrum of Simulated ground motions of Duzce (5% damping).

Table 1: Selected earthquakes.

No	Earthquake	Station	M	D (km)	Vs (m/s)	Duration(s)
01	Spitak, Armenia	Gukasian	6.77	36.19	275	19.90
02	Kocaeli, Turkey	Izmit	7.51	7.21	811	30
03	Duzce, Turkey	Duzce	7.14	6.58	276	25.89
04	Imperial Valley-02	El Centro Array #9	6.95	6.06	213.44	53.76
05	Cape Mendocino	Eureka-Myrtle & West	7.01	41.97	337.46	44
06	Cape Mendocino	Cape Mendocino	7.01	6.96	567.78	30
07	Griva, Greece	Edessa	6.10	33.29	551.3	28.49

Simulation of time histories by SIMQKE II

SIMQKE-II developed by Vanmarcke *et al*. (1999) is used to perform both the conditional simulation and unconditional simulation of ground motion. In the conditional simulation; the simulated ground motions are statically compatible with, or conditioned by, the recorded known ground motion. The statistical independence of the simulated ground motion depends on their correlation between the known and simulated. Figure 2 illustrates the SIMQKE-II procedure steps for simulating spatially correlated earthquake ground motions at required distances. The basic inputs to the SIMQKE-II program are: the locations of the required simulated points, the spectral density functions of the known recorded ground motions windows, the frequency-dependent spatial correlation function, and the known ground motion time history at the recording points.; where, the selected ground motions are subdivided into a sequence of successive time windows, wherein the power spectrum density function (PSDF) for each time window is calculated. In addition, in this study, the site is assumed to be flat and have uniform soil properties so the spatially varying ground motions of each earthquake are assumed to have the same power spectrum density.

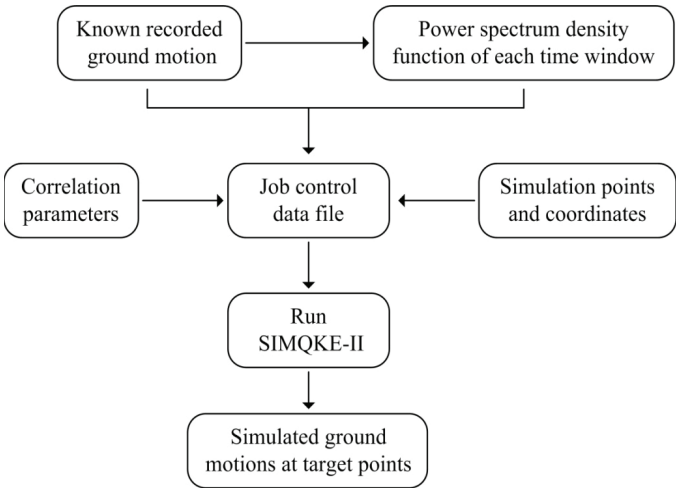

Figure 2. SIMQKE-II procedure steps to simulate spatially correlated earthquake ground motions.

Lagged coherency

The lagged coherency measure the similarity of motions at two different locations (Bi and Hao).The Sobczyk model [14] is selected to describe the coherency loss between the ground motions at points i ' and j ' ($i \neq j$)

$$\gamma_{ij}(i\omega) = \left|\gamma_{ij}(i\omega)\right| \exp(-i\omega_{ij}\cos\alpha / v_{app}) = \exp(-\beta\omega d_{ij}^2 / v_{app}).\exp(-i\omega d_{ij}\cos\alpha / v_{app}) \quad (1)$$

Where, β is a coefficient which reflects the level of coherency loss, β= 0005.0 is used in the present paper, which represents highly correlated motions; d is the distance between the points i' and j', and d_{ij} = 100 m is assumed; α is the incident angle of the incoming wave to the site, and is assumed to be 0°; (as we are not considering any influence of incident angle and the ground motion excitations are applied along longitudinal direction only); v_{app} is the apparent wave velocity in the bedrock, which is 2500 m/s which represent hard rock site condition of the soil. High shear wave velocity is considered to avoid any Soil structure Interaction effect. Figure 3 shows the lagged coherency of the simulated motions. Simulated ground motions showed a good correlation between the known motions which indicates the similarity of simulated motions.

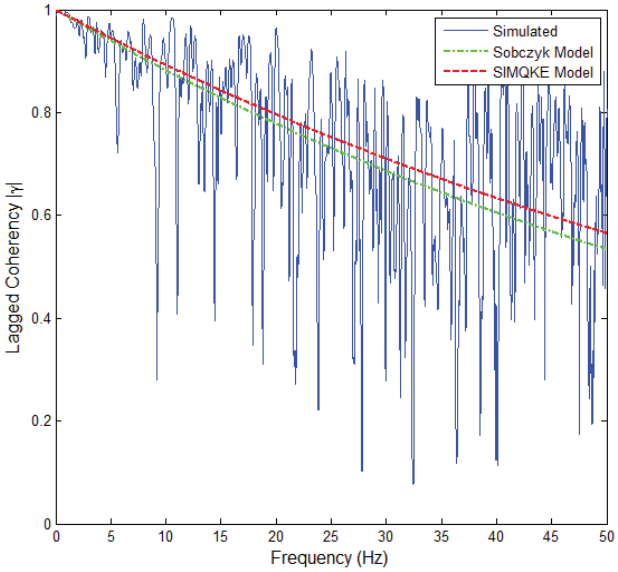

Figure 3. Lagged coherency of Duzce.

Integrated displacement time histories

To get the displacement time histories from the simulated acceleration time histories a high pass filter is applied to the acceleration time histories as suggested by Liao and Zerva where a double integration is applied to the artificial acceleration time histories. After that the displacement time histories were applied at Bi-NPP foundation mat as multi-support excitation along the longitudinal directions. In this study 4th order Butterworth high pass filter was applied (following the approach of Boore et al. 2002) where 98% of the low frequency component with a longer period than the ground motions time history duration are filtered out (suggested by Liao and Zerva). Due to the variance in total time duration of different selected time histories the corner frequencies are different. Figure 4(a) represent the known and simulated acceleration time histories at 0 m, 50 m and 100 m respectively and Figure 4(b) represent their corresponding integrated displacement time histories of Duzce earthquake.

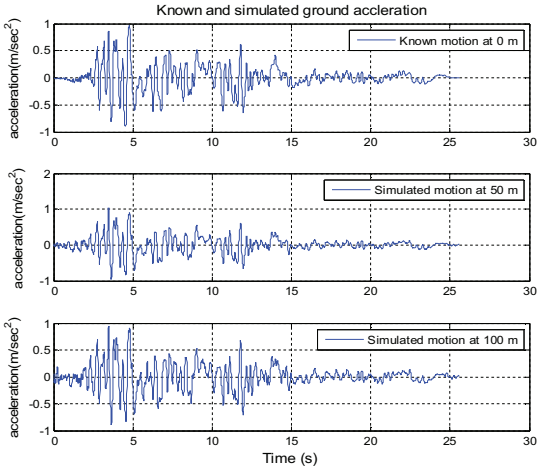

Figure 4: (a) Known And simulated acceleration time history of Duzce.

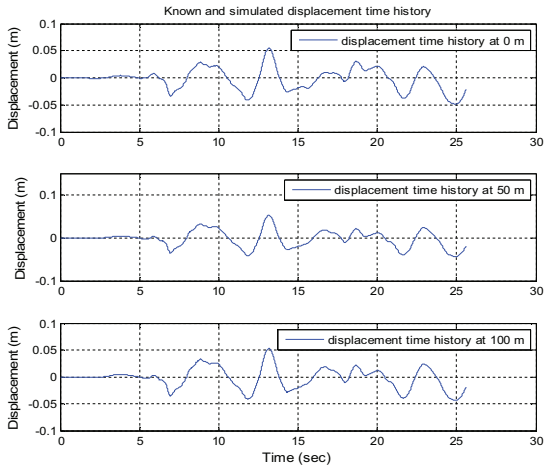

Figure 4: (b) Known And simulated displacement time history of Duzce.

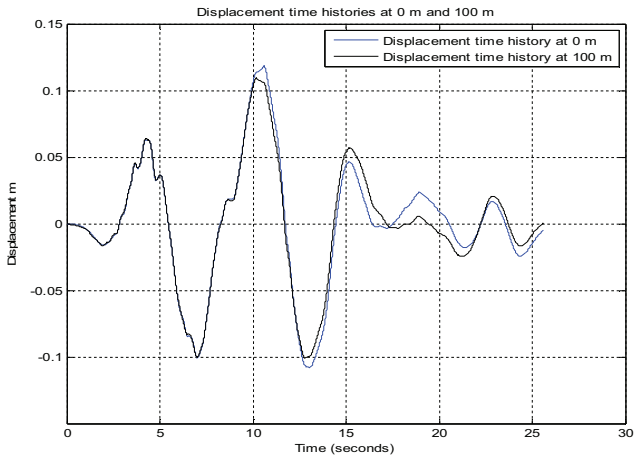

Figure 5. Known and simulated integrated displacement time history at 0 m and 100 m of Spitak.

Where Figure 5 shows that a strong correlation between the displacement time series of Spitak earthquake.

NPP CONTAMINANT BUILDING

The height of the reactor building is 65.8 m and it consists of a cylindrical shell and a hemispherical dome. The lumped mass stick model alongside with the hypothetical structural diagram of the nuclear power plant (APR1000) reactor containment building (Lee and Song 1999) is represented in Figure 6. The stick model of the NPP consists of fourteen nodes and thirteen three-dimensional beam elements with a total height of 65.8 m. The weight of the reactor equipment, steam generators, cranes, etc., is taken into consideration in the lumped masses of the stick model. The actual translational and rotational masses of the NPP are transferred as lumped masses to the corresponding nodes on each element edge.

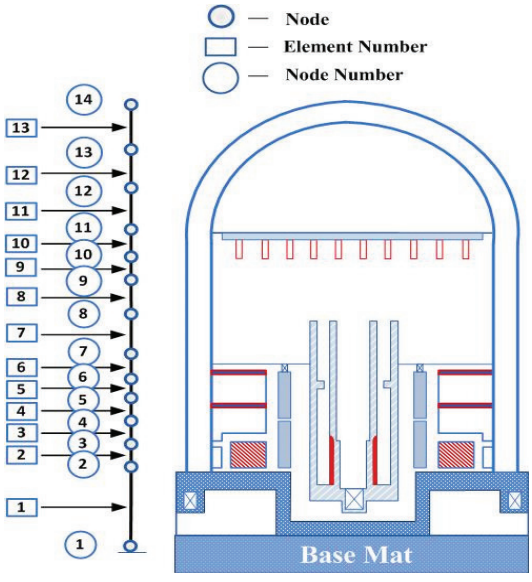

Figure 6. NPP containment building sectional elevation and stick model.

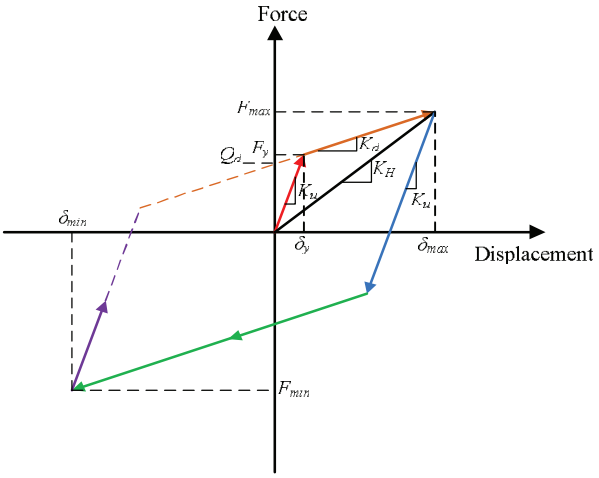

Figure 7. Bi-linear force displacement relationship of the isolators.

Base Isolator

The lead rubber bearing (LRB) base isolation device which has been used for the lateral flexibility of current NPP stick model is composed of low damping natural rubber and a lead plug damper. The rubber is an elastic material. However, the lead plug damper becomes plastic at low levels of stress.The idealised equivalent linear hystereic model of base isolator is shown in figure 7 where the the equivalent linear analysis of the isolator includes the axial stiffness and the equivalent horizontal stiffness of the isolators. Where, K_u is the linear (unloading) horizontal tangential stiffness, K_d is the post-yield horizontal stiffness, and K_H is the effective horizontal stiffness of the isolator. Q_d is the characteristic strength and F_y is the yield strength. δ_{max} is the maximum horizontal displacement, δ_{min} is the minimum horizontal displacement of the isolator; while, F_{max} and F_{min} are the maximum and minimum horizontal forces corresponding to the maximum and minimum horizontal displacements of the isolator, respectively. Table 2 gives the information's about isolator properties and dimensions

Table 2: Properties and dimensions of LRB isolators.

Isolator properties				Isolator dimensions			
Horizontal Stiffness	Post-yielding Stiffness	Yield Strength	Characteristic Strength	Total Thickness rubber layers	Total thickness of the isolator	Lead plug diameter	Outer diameter of isolator
K_H	K_d	F_y	Q_d				
(KN/m)	(KN/m)	(KN)	(KN)	(mm)	(mm)	(mm)	(mm)
8436.10	7089.54	303.73	269.31	180	350	210	1950

The LRB isolator design was designed by adopting the design procedures and requirements of both the Japanese guidelines (*JEA 2000*) and the International Organization for tandardization (ISO) specifications (*ISO 2010*). The isolator stiffness after the lead plug damper yielding is considered as the isolator key performance indicator.

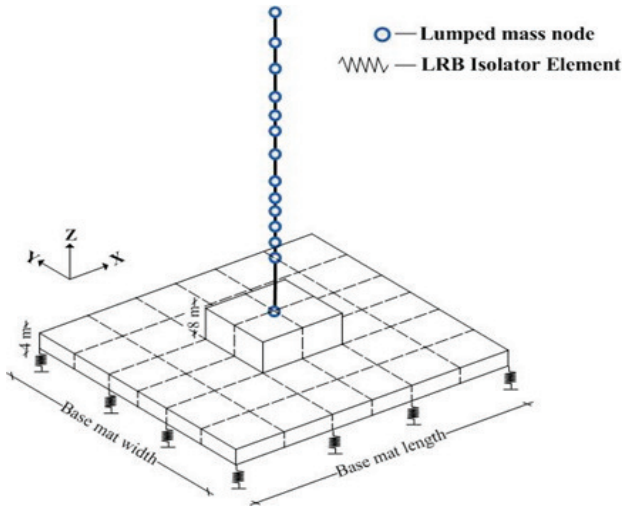

Figure 8. (a) Base mat dimensions of stick model.

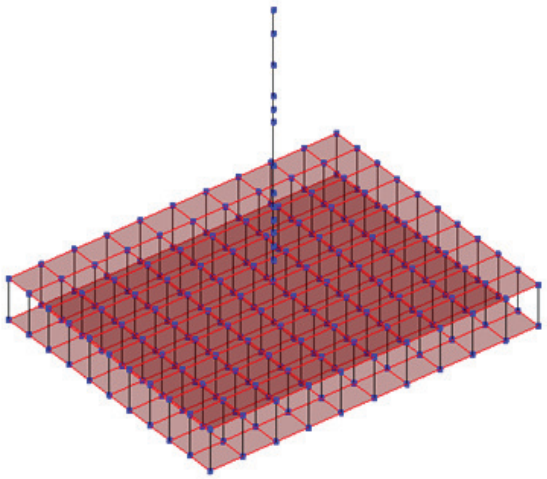

Figure 8. (b) BI-NPP with 121 isolators.

In this study, total masses of the BI-NPP considered 110,950 tons for designing isolators where table: 3 desscribes the base mat dimensions along with the distributions of number of isolators along two horizontal directions and figure 8 (a) & (b) represent the same.

Table 3: Base mat dimensions and isolator numbers.

Base mat dimensions			No. of LRB isolators		Total no. of isolators
Length (m)	Width (m)	Area (m^2)	along X-dir.	along Y-dir.	
100	80	8000	11	11	121

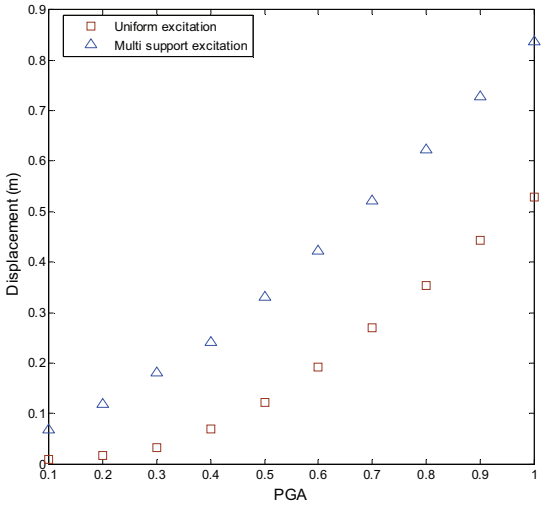

Figure 9. Mean displacement responses for both uniform and multi-support excitation.

Fixed base structures have different major modes shape dominating the frequency range and natural period of the responses. But Base Isolated structures shows its major response for first mode shape and it does not contain different major frequencies. Base Isolated structures are nonlinear and for them displacements of isolators' node is the most critical criterion to be considered. Besides the inter story drift of base-isolated nuclear power plant do not change dramatically compared to NPP. Hence displacements at isolator node is considered as paramount structural response of BI-NPP. Figure 9 represents the mean of maximum displacements obtained by analysis from PGA 0.1 to 1.

FRAGILITY CURVES

This Study uses multiple stripe analysis (MSA) where no need to perform analysis up to specific intensity measure amplitude where all ground motion cause collapse which is briefly summarized here. A lognormal cumulative distribution function is used to define a fragility function

$$P = \Phi\left(\frac{\ln(x/\theta)}{\beta}\right) \tag{2}$$

Where, P is the probability that a ground motion with $PGA = x$ will cause the structure to collapse, $\Phi(\ )$ is the standard normal cumulative distribution function (CDF), θ is the median of the fragility function and β is the standard deviation of lnPGA. PGA values of ground motions are log normally distributed. At

each intensity level $PGA = x_j$, the structural analyses produce some number of collapses out of a total number of ground motions. The probability of observing z_j collapses out of n_j ground motions with $PGA = x_j$ is given by the binomial distribution

$$P = \binom{n_j}{z_j} p_j^{z_j} (1 - p_j)^{n_j - z_j} \tag{3}$$

Where, P is the probability of z_j collapses out of n_j ground motions p_j is the probability that a ground motion with $PGA = x_j$, will cause collapse of the structure. After getting the analysis data at several PGA levels the product of binomial probabilities at each PGA level for the entire data set is given by

$$\text{Likelihood} = \prod_{j=1}^{m} \binom{n_j}{z_j} p_j^{z_j} (1 - p_j)^{n_j - z_j} \tag{4}$$

Where, m is the number of PGA levels and Π denotes the product over all levels. Now substituting the equation 3 for p_j, the likelihood function is

$$\text{Likelihood} = \prod_{j=1}^{m} \binom{n_j}{z_j} \Phi\left(\frac{\ln\left(x_j / \theta\right)}{\beta}\right)^{z_j} \left(1 - \Phi\left(\frac{\ln(x_j / \theta)}{\beta}\right)\right)^{n_j - z_j} \tag{4}$$

The maximization of this likelihood function is required to get the estimate of fragility function parameters where logarithmic maximization is adopted for numerical simplicity and the following equation is used finally to get fragility parameters. (J. Baker 2013)

$$\left\{\hat{\theta}, \hat{\beta}\right\} = \arg\max_{\theta,\beta} \sum_{j=1}^{m} \left\{ \ln\binom{n_j}{z_j} + z_j \ln \Phi\left(\frac{\ln(x_j / \theta)}{\beta}\right) + (n_j - z_j) \ln\left(1 - \Phi\left(\frac{\ln(x_j / \theta)}{\beta}\right)\right)\right\} \tag{4}$$

Where, $\hat{\theta}$ and $\hat{\beta}$ denotes the median and lognormal standard deviation respectively for calibration of equation 3. After getting the analysis data and making the use of equation 7 fragility curve is constructed.

The maximum displacement responses obtained from the isolator node is taken into consideration for fragility analysis. For each set of ground motions, three limit state values corresponding to 0.5, 1.0 and 1.5 times the allowable displacements D_D (which is 200 mm) are used to obtain the fragility curve i.e., a family of three fragility curve will be plotted for $0.5*D_D$ (Limit State-I), $1*D_D$ (Limit State-II) *and* $1.5*D_D$ (Limit State-III)respectively. Figure 10 and figure 11 represent the fragility curves for spatially varied ground motion and uniform ground motion respectively. It is clearly visible that differential ground motion is giving a steeper result compared to identical support ground motion.

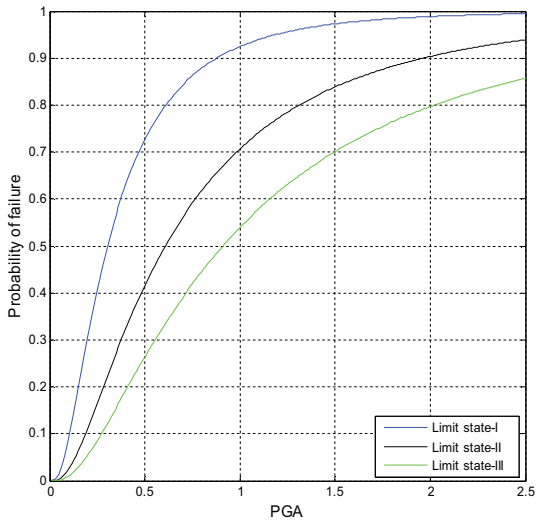

Figure 10. Fragility curve for spatially varied ground motion.

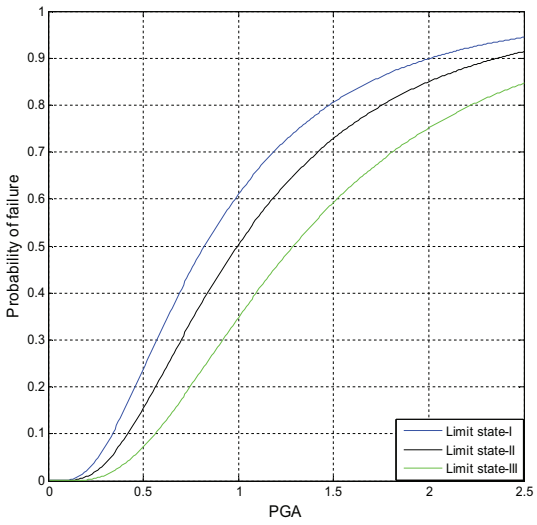

Figure 11. Fragility curve for uniform ground motion excitation.

CONCLUSION

Fragility curves were developed of base-isolated NPP subjected to uniform and spatially varying ground motion for three different limit states of design displacement by nonlinear time history analysis for each ground motion scaled with different incremental PGA values to get the displacement responses of isolator node for every seismic inputs. Three different limit states for which fragility i.e. probability of failure is estimated at each ground motion excitation level are $0.5*D_D$ (Limit State-I), $1*D_D$ (Limit State-II) *and* $1.5*D_D$ (Limit State-III) respectively where D_D is the allowable displacement of base isolator node .The maximum displacement of the isolator node is then taken as prime structural response. The analytical fragility curve is constructed using the multiple stripe analysis where observed collapse numbers are counted utilizing the maximum likelihood function.

The study found that the BI-NPP is susceptible enough for spatially ground motion than uniform excitation and the developed fragility curves are consistent with this hypothesis for all limit states. The number of collapse were observed for each limit states and it was found that number of collapse for multi support excitation in each analysis in each PGA level is considerably higher.

A family of three fragility curves for three design limit states were plotted, showed that the rate of change of failure probability is different i.e., a linear change in design limit dose not yield a linear change in failure probability. This study found that spatial variation effect results 2.3 times collapse for limit state-I, 1.9 times for limit state-II and 2.5 times for limit state-III compared to uniform ground motions.

Finally a practical seismic design code is recommended where structures will be analysed accounting spatially varying ground motion effect consistently. Nevertheless every probabilistic seismic performance based assessment should account the differential ground motion effect reflecting wave passage effect, incoherence effect and local site effect. Because conventional uniform excitation may result less conservative and overestimate the structural capacity.

ACKNOWLEDGEMENT

This work was supported by the Nuclear power Core Technology Development Program of the Korea Institute of Energy Technology Evaluation and Planning (KETEP) grant financial resource from the Ministry of Trade, Industry & Energy, Republic of Korean (No. 2014151010170A).

REFERENCES

Shinozuka M., Deodatis G. and Saxena V. (2000). "Effect of spatial variation of ground motion on bridge response," Technical Report MCEER-00-0013.

Kim S.H. & Feng M.Q, (2003). "Fragility analysis of bridges under ground motion with spatial variation," International Journal of Non-Linear Mechanics, 38 705-721.

Cho Sung Gook and Joe Yang Hee. (2005). "Seismic fragility analyses of nuclear power plant structures based on the recorded earthquake data in Korea," Nuclear Engineering and Design, 235 1867-1874.

Ali A., Nadine A.H, Kim D, Cho S.G. (2014). "Probabilistic Seismic Assessment of Base-Isolated NPPs Subjected To Strong Ground Motions of Tohoku Earthquake," Nuclear Engineering and Technology, 46(5) 699-706.

United States Nuclear Regulatory Commission (USNRC). (2012). "Standard review plan for the review of safety analysis reports for nuclear power plants, 3.7.1. Seismic design Parameters," NUREG-0800, USNRC, Washington, USA.

Vanmarcke, E.H., Fenton, G.A. and Heredia-Zavoni, E. (1999). "Conditioned earthquake ground motion simulator," SMIQKE-II User's manual, version 2.1.

Bi, K. and Hao, H. (2012). "Modelling and simulation of spatially varying earthquake ground motions at sites with varying conditions," Probabilistic Engineering Mechanics, 29 92-104.

Boore, D.M., Stephens, C.D. and Joyner, W.B. (2002). "Comments on baseline correction of digital strong motion data: Examples of the 1999 Hector Mine, California, Earthquake," Bulletin of the Seismological Society of America, 92 1543-1560.

Japan Electric Association (JEA), (2000). "Design and technical guideline of seismic isolation structure for nuclear power plant," Nuclear Standard Committee of JEA, JEAG 4614-2000, (in Japanese only).

Schellenberg, A., Yang, T.Y. and Kohama, E. (2013). OpenSees Navigator 2.5.2, https://nees.org/resources/osnavigator.

International Standard Organization (ISO), (2010). "Elastomeric seismic-protection isolators-part 3: Applications for buildings-specifications," ISO 22762-3:2010.

Baker, J. W. (2013). "Efficient analytical fragility function fitting using dynamic structural analysis. Earthquake Spectra," https://web.stanford.edu/~bakerjw/fragility.html .

Sayed, M.A. (2014). "The Effect of Spatial Variation of Earthquake Ground Motions on the Seismic Responses of a Base-Isolated Nuclear Power Plant," MSc. Dissertation, Dept. of Civil & Environment Engineering, Kunsan National University, South Korea.

Huang Y.N., Whittaker A.S. and Luco N., (2008). "Seismic Performance Assessment of Nuclear Power Plants," Proc., 14th World Conference on Earthquake Engineering.

Zerva, A. (2009). "Spatial Variation of Seismic Ground Motions: Modeling and Engineering Applications," Taylor & Francis Group, CRC Press, Florida, USA.

Liao, S. and Zerva, A. (2006). "Physically-compliant, conditionally simulated spatially variable seismic ground motions for performance-based design," Earthquake Engineering and Structural Dynamics, 35 891-919.

PEER strong ground motion Database, "https://ngawest2.berkeley.edu/".